Solvent Effects on Raman Optical Activity Spectra Calculated Using the Polarizable Continuum Model

Magdalena Pecul* and Ewa Lamparska

Department of Chemistry, University of Warsaw, Pasteura 1, 02-093 Warsaw, Poland

Chiara Cappelli

PolyLab-CNR-INFM, c/o Dipartimento di Chimica e Chimica Industriale, Universitá di Pisa, Via Risorgimento 35, 56126 Pisa, Italy

Luca Frediani and Kenneth Ruud

Department of Chemistry, University of Tromsø, N-9037 Tromsø, Norway

Received: November 8, 2005; In Final Form: December 13, 2005

The integral equation formulation of the polarizable continuum model (IEFPCM) has been extended to the calculation of solvent effects on vibrational Raman optical activity spectra. Gauge-origin independence of the differential scattering intensities of right and left circularly polarized light is ensured through the use of London atomic orbitals. Density functional theory (DFT) calculations have been carried out for bromochlorofluoromethane, methyloxirane, and epichlorhydrin. The results indicate that solvent effects on the ROA differential scattering intensities can be substantial, and vary in sign and magnitude for different vibrational modes. It is demonstrated that both direct and indirect effects are important in determining the total solvent effects on the ROA differential scattering intensities. Local field effects are shown to be in general small, whereas electronic nonequilibrium solvation has a profound effect on the calculated solvent effects compared to an equilibrium solvation model. For molecules with several conformations, the changes in the relative stability of the different conformers also lead to noticeable changes in the ROA spectra.

I. Introduction

There is currently an increasing interest in calculations of vibrational Raman optical activity (ROA) using quantum chemical methods;[1−6] see also ref 7 for a review. This can in part be attributed to the potential of ROA for use in biochemistry as a way of determining the spatial structure of biomolecules[8−13] and in pharmaceutical chemistry as a tool for establishing absolute configuration and enantiomeric purity of biologically active compounds.[13] ROA and a complementary technique, vibrational circular dichroism (VCD), are much more powerful approaches for these purposes than electronic circular dichroism (ECD), since more data are available for each molecule due to the much higher number of accessible vibrational modes compared to the number of excited states observable in ECD. Moreover, VCD and ROA can be applied to molecules lacking suitable electronic chromophores which are therefore inaccessible to ECD.

In studies of molecular conformations and determination of absolute configurations, quantum chemical calculations can be very useful, provided a direct comparison between theory and experiment is possible. However, in the case of ROA, such a comparison is problematic. Experimental studies of ROA are difficult due to the small differences in scattering of right and left circularly polarized light. Moreover, ROA spectra have so far only been collected in condensed phases, either in neat liquids or, in the case of biomolecules, in aqueous solutions. It is well-known that molecular properties associated with chirality are sensitive to solvent effects. For instance, the optical rotation has been reported to change sign when changing the solvent, even for rigid molecules.[14,15] ROA intensities can also be expected to depend strongly on the solvent considering their strong sensitivity to other perturbations such as conformational changes.[16] Therefore, accounting for solvent effects by means of an inexpensive and reliable computational model is important if theoretically calculated ROA spectra are to be used for interpretation and prediction of experimental spectra.

The polarizable continuum model (PCM),[17−19] in which the solvent is represented as an infinite, homogeneous, and polarizable dielectric medium and the solute molecule is placed in a molecule-shaped cavity in this medium, is a popular solvent model which is computationally inexpensive, and conceptually simple. Although PCM has been originally designed to treat heterogeneous solvation, there are strategies developed to treat additional solvent effects that may be relevant in the case of pure liquids; see for example refs 20 and 21. These methods can also be extended to treat solvent effects on ROA. The intrinsic limitation of the basic formulation of PCM is the lack of solvent−solute interactions which are not purely electrostatic in nature (such as hydrogen bonds or dispersion interactions). These limitations can be rectified by introducing explicit solvent molecules, which however increases the computational cost of the calculation. In many cases, this makes such calculations prohibitively expensive, especially for those which are very time-consuming even for molecules in the gas phase, such as the calculation of ROA scattering intensity differences. Despite the inherent limitations in the PCM, the model has been

* Corresponding author, e-mail mpecul@chem.uw.edu.pl.

10.1021/jp056443c CCC: $33.50
Published on Web 02/08/2006

demonstrated to reproduce satisfactorily experimental solvent effects for several molecular properties[19] (among them spin−spin coupling constants[22]) and solutions, including the study of neat liquids. PCM has recently been used to calculate a number of optical properties such as optical rotation,[23] electronic circular dichroism,[24] vibrational circular dichroism,[25] and Raman spectra.[26] In this paper, we present the extension of PCM to the calculation of ROA spectra.

In the present work, the IEFPCM (integral equation formalism polarizable continuum model) approach to solvent effects on ROA circular scattering intensity differences is applied to bromochlorofluoromethane, methyloxirane, and epichlorhydrin—all of which are small, rigid molecules often used as test molecules in calculations of chiroptical properties.[24,27−29] Solvent effects on the ROA spectrum of methyloxirane are interesting in their own right, since it has been reported that both the optical rotation[14] and the ECD spectrum[24] of this molecule are very sensitive to the choice of solvent. It is in particular of interest to predict whether solvent-induced changes in the ROA intensities for all vibrations of a given molecule go in the same direction, following the changes in the optical tensors, or go in different directions. In the latter case, solvent effects on ROA spectra would be much easier to detect experimentally, and they would be of more practical importance. Another aspect of the present work is to gain insight into the methodological aspects of PCM calculations of ROA spectra, such as how much of the total solvent effect comes from the changes in the optical tensors ("direct" effects), how much originates from changes in the molecular Hessian ("indirect" effects) and how important it is to account for "local field" effects (see below). For this purpose, the effect of the dielectric medium on the optical tensors and on the force field were considered separately. This is particularly relevant in connection with earlier studies by Jalkanen and coworkers[30,31] which addressed only dielectric medium effects on the ROA spectrum through changes in the force field ("indirect" effects) and included, in certain cases, also explicit water molecules in addition to a dielectric continuum.[30,31] The present study is the first complete investigation of solvent effects modeled using a dielectric continuum model on ROA circular scattering intensity differences. We therefore use this opportunity also to study other methodological aspects of the calculations, such as the use of equilibrium and nonequilibrium solvation models.

The remainder of the paper is organized as follows. In section II, the theory of ROA calculations and of PCM is briefly discussed, and in section III the computational details are given. In section IV, the calculated ROA spectra of (*R*)-bromochlorofluoromethane, (*S*)-methyloxirane, and (*S*)-epichlorhydrin in gas phase and in solution are presented and discussed. Finally, we give in section V a brief summary of our results and some concluding remarks.

II. Theory

A. Raman Optical Activity. The quantity of interest in ROA is the differential scattering intensity between right and left circularly polarized light $I_k^R - I_k^L$ [32,33]

$$\Delta_k = I_k^R - I_k^L \tag{1}$$

where $I_k^{L,R}$ are the scattered intensities with linear *k* polarization for right (R) and left (L) circularly polarized incident light, and *k* denotes the Cartesian component. Following Helgaker et al.,[34] and for the time being ignoring solvent effects, the differential scattering intensities between right and left circularly polarized light for the polarized right-angle scattering of Raman optical activity is given by

$$\Delta_z(90) = 6\beta(G')^2 - 2\beta(A)^2 \tag{2}$$

where

$$\beta(G')^2 = \frac{3\alpha^{o}_{ki}G'^{o}_{ki} - \alpha^{o}_{kk}G'^{o}_{ii}}{2} \tag{3}$$

$$\beta(A)^2 = \frac{1}{2}\omega_{rad}\alpha^{o}_{ki}\epsilon_{kjl}A^{o}_{jli} \tag{4}$$

ω_{rad} is the radiation angular frequency, ϵ_{kjl} is the unit third rank antisymmetric tensor and the other quantities are within the Placzek approximation[35] defined as

$$\alpha^{o}_{ki}G'^{o}_{ki} = \langle 0|\alpha_{ki}|1\rangle\langle 1|G'_{ki}|0\rangle = \frac{1}{2\omega}\left(\frac{\partial\alpha_{ki}}{\partial Q}\right)_0\left(\frac{\partial G'_{ki}}{\partial Q}\right)_0 \tag{5}$$

$$\alpha^{o}_{ki}\epsilon_{kjl}A^{o}_{jli} = \langle 0|\alpha_{ki}|1\rangle\langle 1|\epsilon_{kjl}A_{jli}|0\rangle = \frac{1}{2\omega}\left(\frac{\partial\alpha_{ki}}{\partial Q}\right)_0\epsilon_{kjl}\left(\frac{\partial A_{jli}}{\partial Q}\right)_0 \tag{6}$$

Implicit summation over repeated indices is used throughout the paper. The tensors in eqs 5−6 are the electric dipole−electric dipole polarizability $\boldsymbol{\alpha}$, the imaginary part of the electric dipole−magnetic dipole polarizability $\mathbf{G}'$, and the real part of the electric dipole−electric quadrupole polarizability $\mathbf{A}$.[34] ω is the frequency associated with the vibrational transition and Q is the corresponding normal coordinate. The subscript 0 indicates that the quantities are calculated at the equilibrium geometry. We note that the mixed electric dipole−magnetic dipole and the electric dipole−electric quadrupole polarizabilities individually depend on a choice of origin. The origin dependence of the two contributions cancels in the anisotropic invariants. However, in approximate calculations using finite basis sets, this cancellation of the origin dependence can only be achieved through the use of London atomic orbitals,[36] as demonstrated in ref 34. Consequently, all calculations reported in this paper use London orbitals, following previous work for optical rotation calculations for solvated molecules.[23,37]

B. Solvent Effects on ROA: The Polarizable Continuum Model Approach. The extension of the theory presented above to systems in condensed phase requires some preliminary considerations. In fact, in addition to considering "direct" solvent effects, i.e. the solvent effects on the solute electronic density (here affecting all the polarizability terms as well as the vibrational states and thus the normal coordinates), it should also be taken into consideration that the solvent reaction field perturbs the molecular geometry of the solute, and thus all quantities defined in eqs 5 and 6 are to be calculated at the solute equilibrium geometry on the solvated potential energy surface (PES). The calculation of "direct" effects, as well as of the PES in solution, must be done using a suitable solvation model, and in this paper, IEFPCM is used.[38] In PCM the solvent is modeled as an infinite, homogeneous, and usually isotropic dielectric medium, characterized by a dielectric constant ϵ, surrounding a solute which is hosted in a molecule-shaped cavity. The evaluation of the energy arising from the electrostatic interaction between the solute and the solvent, including also mutual polarization effects, is obtained by introducing an apparent surface charge defined on the cavity boundary.

To obtain a realistic description of the response of the electronic density of the solute to an applied electromagnetic field—and consequently on the spectroscopic properties of the molecule—we need to take into account that in continuum

solvation models, the electric field acting on the molecule in the cavity is different from the Maxwell field in the dielectric. The response of the solute to the external perturbation depends only on the local electromagnetic field experienced by the molecule. This is usually referred to as a "local field" effect and is normally solved by resorting to the Onsager−Lorentz theory of dielectric polarization,[39,40] which considers the solute simply as a polarizable point dipole in a spherical cavity in the dielectric. A quantum mechanical approach to the "local field" problem has been formulated for PCM for several optical and spectroscopic properties.[20,21,25,26,41−44]

The foundations for the PCM approach to the "local field" problem rely upon the assumption that the "effective" field experienced by the molecule in the cavity can be seen as the sum of a reaction field term and a cavity field term. The reaction field is connected to the response (polarization) of the dielectric to the solute charge distribution, whereas the cavity field depends on the polarization of the dielectric induced by the applied field once the cavity has been created.

In analogy with Onsager's theory of electric polarization, it is assumed that the response of the molecule to the external probing field can be expressed in terms of an "effective dipole moment"

$$\boldsymbol{\mu}^* = \boldsymbol{\mu} + \tilde{\boldsymbol{\mu}} \tag{7}$$

where $\boldsymbol{\mu}$ is the molecular dipole moment and $\tilde{\boldsymbol{\mu}}$ is the dipole moment arising from the molecule-induced dielectric polarization. Using this assumption, the quantities analogous to those reported in eqs 2−6 for systems in solution are

$$(I_z^{\mathrm{R}} - I_z^{\mathrm{L}})^{\mathrm{sol}}(90) = 6\tilde{\beta}(G')^2 - 2\tilde{\beta}(A)^2 \tag{8}$$

$$\tilde{\beta}(G')^2 = \frac{3\tilde{\alpha}^{o}_{ki}\tilde{G}'^{o}_{ki} - \tilde{\alpha}^{o}_{kk}\tilde{G}'^{o}_{ii}}{2} \tag{9}$$

$$\tilde{\beta}(A)^2 = \frac{1}{2}\omega_{\mathrm{rad}}\tilde{\alpha}^{o}_{ki}\epsilon_{kjl}\tilde{A}_{jli} \tag{10}$$

$$\tilde{\alpha}^{o}_{ki}\tilde{G}'^{o}_{ki} = \langle 0_{\mathrm{sol}}|\tilde{\alpha}_{ki}|1_{\mathrm{sol}}\rangle\langle 1_{\mathrm{sol}}|\tilde{G}'_{ki}|0_{\mathrm{sol}}\rangle = \frac{1}{2\omega_{\mathrm{sol}}}\left(\frac{\partial\alpha^*_{ki}}{\partial Q_{\mathrm{sol}}}\right)_0\left(\frac{\partial\tilde{G}'_{ki}}{\partial Q_{\mathrm{sol}}}\right)_0 \tag{11}$$

$$\tilde{\alpha}^{o}_{ki}\epsilon_{kjl}\tilde{A}_{jli} = \langle 0_{\mathrm{sol}}|\tilde{\alpha}_{ki}|1_{\mathrm{sol}}\rangle\langle 1_{\mathrm{sol}}|\epsilon_{kjl}\tilde{A}_{jli}|0_{\mathrm{sol}}\rangle = \frac{1}{2\omega_{\mathrm{sol}}}\left(\frac{\partial\alpha^*_{ki}}{\partial Q_{\mathrm{sol}}}\right)_0\epsilon_{\mathrm{kjl}}\left(\frac{\partial\tilde{A}_{jli}}{\partial Q_{\mathrm{sol}}}\right)_0 \tag{12}$$

In these equations, $\boldsymbol{\alpha}^*$ is the "effective" Raman electric dipole−electric dipole polarizability,[26] $\tilde{\mathbf{G}}'$ is the imaginary part of the "effective" electric dipole−magnetic dipole polarizability, and $\tilde{\mathbf{A}}$ the real part of the "effective" electric dipole−electric quadrupole polarizability, all containing both reaction field and cavity field effects. The definitions of the quantities above are

$$\alpha^*_{ki} = 2\sum_{r\neq l}\frac{\omega_{rl}\mathrm{Re}[\langle l|\mu_k + \tilde{\mu}_k|r\rangle\langle r|\mu_i + \tilde{\mu}_i|l\rangle]}{\omega_{rl}^2 - \omega_{\mathrm{rad}}^2} \tag{13}$$

$$\tilde{G}'_{ki} = -2\omega_{\mathrm{rad}}\sum_{r\neq l}\frac{\mathrm{Im}[\langle l|\mu_k + \tilde{\mu}_k|r\rangle\langle r|m_i|l\rangle]}{\omega_{rl}^2 - \omega_{\mathrm{rad}}^2} \tag{14}$$

$$\tilde{A}_{kil} = 2\sum_{r\neq l}\frac{\omega_{rl}\mathrm{Re}[\langle l|\mu_k + \tilde{\mu}_k|r\rangle\langle r|\Theta_{il}|l\rangle]}{\omega_{rl}^2 - \omega_{\mathrm{rad}}^2} \tag{15}$$

m is the magnetic dipole operator and Θ the traceless electric quadrupole moment operator. The presence of $\tilde{\mu}$ introduces the cavity field effects. A formulation of this operator in the PCM scheme has been reported elsewhere.[21,43] Suffice it to mention here that this operator can be expressed in terms of a suitable set of point charges (the external charges) q^{ex}, each associated with a portion (tessera) of the cavity surface so that, by using standard boundary element method techniques

$$\tilde{\mu} = -\left(\sum_l V(\mathbf{s}_l)\frac{\partial q_l^{\mathrm{ex}}}{\partial \mathbf{E}}\right) \tag{16}$$

where $V(\mathbf{s}_l)$ is the electric potential associated with the molecular charge density, measured at the center of the l'th tessera $\mathbf{s}_l$, and $\mathbf{E}$ is the Maxwell electric field. The charges q^{ex} are calculated using the standard PCM relation[45]

$$\mathbf{q}^{\mathrm{ex}} = -\mathbf{D}^{-1}\mathbf{e}_{\mathbf{n}} \tag{17}$$

where the PCM $\mathbf{D}$ matrix is calculated from the optical dielectric constant of the medium, thus taking into account the solvent nonequilibrium response to the external electric field (electronic nonequilibrium, see below), and where $\mathbf{e}_{\mathbf{n}}$ collects the components of the external electric field normal to the cavity surface.[41,43]

Resorting to the linear response framework,[46,47] the tensors in eqs 13−15 may be expressed as response properties by a proper choice of operators. More specifically

$$\alpha^*_{ki} = -\langle\langle\mu^*_k; \mu^*_k\rangle\rangle_{\omega_{\mathrm{rad}}} \tag{18}$$

$$\tilde{G}'_{ki} = -\langle\langle\mu^*_k; m_i\rangle\rangle_{\omega_{rad}} \tag{19}$$

$$\tilde{A}_{kil} = -\langle\langle\mu^*_k; \Theta_{il}\rangle\rangle_{\omega_{\mathrm{rad}}} \tag{20}$$

We note that the PCM approach to the calculation of $\partial\alpha^*_{ki}/\partial Q_{\mathrm{sol}}$ has already been reported for Raman scattering in ref 26.

It is worth noticing that in the case of ROA (as well as Raman) spectra, a complete treatment of the dynamics of the solvent molecules (the so-called "nonequilibrium effects") should involve the consideration of two distinct effects: the dynamic (nonequilibrium) response of the solvent to the external field-induced oscillation in the solute electronic density (electronic nonequilibrium) and the dynamics of the solvent due to solute vibrational motions (vibrational nonequilibrium). A formulation of both these effects for Raman spectra has previously been reported.[48] In this paper, only the "electronic nonequilibrium effects" are considered, whereas we assume that the solvent is always equilibrated to the solute charge distribution of the unperturbed momentary nuclear configuration—that is, vibrational nonequilibrium effects will not be considered. This approximation can be expected to be acceptable—even though vibrational nonequilibrium effects have been shown to give substantial corrections to infrared absorption intensities of molecules in solution[49]—since these effects are in general negligible for Raman intensities.[48]

III. Computational Details

The geometry optimization was carried out using density functional theory with the hybrid Becke three-parameter Lee−Yang−Parr (B3LYP) functional[50,51] with the cc-pVTZ basis set.[52,53] The force field for the ROA calculation was obtained at the same level of theory. Optical tensors were calculated using DFT/B3LYP and the aug-cc-pVDZ basis[52−55] set, since in this

TABLE 1: Vibrational Frequencies $\bar{\nu}$ and Differential Scattering Intensities of Right and Left Circularly Polarized Light ($I^R - I^L$, Arbitrary Units) Calculated for Methyloxirane in the Gas Phase (Gas, Gas), Using Force Field as In Acetonitrile and Optical Tensors from the Gas Phase (Sol, Gas), Force Field from the Gas Phase and Optical Tensors as in Acetonitrile (Gas, Sol), and Both Force Field and Optical Tensors as In Acetonitrile, Where Noncf and Static Indicate Neglect of Cavity Field Corrections and the Use of Static (Equilibrium) Solvation, Respectively

	$\bar{\nu}_{gas}$ [cm^{-1}]	gas, gas	gas, sol	$\bar{\nu}_{sol}$ [cm^{-1}]	sol, gas	sol, sol	noncf	static
1	3158.7	0.070	0.043	3163.4	0.136	0.104	0.153	0.060
2	3116.4	0.444	0.315	3099.8	0.238	−0.020	−0.024	−0.036
3	3093.7	−0.272	−0.259	3081.0	−0.145	−0.129	−0.141	−0.081
4	3081.9	−0.076	−0.028	3076.4	−0.119	−0.103	−0.099	−0.087
5	3072.1	−0.053	−0.042	3074.3	0.208	0.209	0.217	0.203
6	3037.6	−0.007	−0.023	3016.6	−0.001	0.002	0.002	−0.001
7	1535.6	−0.472	−0.449	1521.6	−0.430	−0.446	−0.580	−0.268
8	1496.5	0.861	0.640	1486.1	0.937	0.802	0.920	0.521
9	1482.0	−0.210	−0.179	1473.2	−0.240	−0.290	−0.191	−0.150
10	1439.4	−0.251	−0.182	1433.6	−0.266	−0.169	−0.180	−0.118
11	1413.2	0.185	0.246	1401.7	0.337	0.406	0.399	0.276
12	1295.1	0.063	0.052	1289.8	0.063	0.068	0.064	0.053
13	1187.2	−0.654	−0.677	1186.6	−0.509	−0.555	−0.635	−0.482
14	1165.2	0.365	−0.202	1164.1	0.230	−0.264	−0.112	−0.523
15	1156.7	0.606	0.739	1152.8	0.443	0.526	0.530	0.441
16	1127.9	−0.258	−0.629	1123.9	−0.280	−0.563	−0.501	−0.501
17	1045.2	0.335	0.978	1039.7	0.582	0.974	0.935	0.962
18	968.5	0.162	0.080	964.0	0.184	0.167	0.142	0.193
19	914.9	−0.709	−0.519	906.0	−0.803	−0.737	−0.762	−0.648
20	845.9	−0.300	−0.312	832.3	−0.307	−0.336	−0.335	−0.336
21	774.9	0.194	0.382	758.6	0.201	0.392	0.347	0.494
22	413.5	−0.058	0.149	409.8	−0.093	0.115	−0.200	0.553
23	366.0	−0.499	−0.468	367.5	−0.473	−0.310	−0.393	0.280
24	195.8	−0.464	0.105	210.8	−0.237	−0.152	0.278	0.438

case the presence of diffuse functions should be more important for the quality of the calculations than higher angular momentum functions. This basis set has also been shown to be a good compromise between accuracy and computational cost in calculations of ROA spectra.[6]

The radii of the spheres used to build the molecule-shaped cavity for methyloxirane and epichlorhydrin were 2.40 Å for CH_2 and CH_3 groups, 2.28 Å for the CH group, 1.82 Å for the oxygen atom, and 2.40 Å for the chlorine atom. For bromochlorofluoromethane, the radii 2.04, 1.44, 1.62, 2.17, and 2.34 Å were used for C, H, F, Cl, and Br, respectively. The spheres used are based on the modified Bondi radii[56] and united-atom type model, similar to that reported in ref 57. Calculations were performed in cyclohexane and acetonitrile using the optical (opt) and static (0) dielectric constants $\epsilon_{opt} = 2.028$, $\epsilon_0 = 2.023$ for cyclohexane and $\epsilon_{opt} = 1.806$, $\epsilon_0 = 36.64$ for acetonitrile. All calculations were performed using a local version of the DALTON program package[58] containing the PCM code. Raman and ROA spectra were obtained by numerical differentiation of optical tensors with respect to the nuclear coordinates.

IV. Results and Discussion

As already discussed in the Introduction, solvent effects on ROA intensities can be divided into contributions originating from the molecular Hessian (i.e. geometry changes induced by the medium), and direct effects on the optical tensors. Only the former of these effects have so far been considered in the literature.[30,31] Before discussing the total changes of the ROA spectra in different solvents, we will consider these contributions separately.

Table 1 contains vibrational frequencies and differential scattering intensities of right and left circularly polarized light of (*S*)-methyloxirane in gas phase (gas,gas) and in acetonitrile solution, calculated using three approaches: molecular Hessian in gas phase and optical tensors calculated in solution (gas, sol), a procedure which only accounts for direct solvent effects, molecular Hessian calculated in solution and optical tensors in gas phase (sol, gas), accounting only for indirect solvent effects, and finally both molecular Hessian and optical tensors calculated in solution accounting for both direct and indirect solvent effects.

We note from the data in Table 1 that it is essential to account for both indirect and direct effects in PCM calculations of solvent effects on ROA spectra. There are some vibrations, such as for example the symmetric stretching of the CH_2 group (mode 5), where the indirect contribution (from the molecular Hessian) to the solvent effect is by far dominant (0.209 vs −0.042 with respect to −0.053 vs −0.042), but there are also opposite cases, such as the C−H bending modes 16 and 17 where the total solvent effect originates mostly from the direct influence of the dielectric environment on the optical tensors (compare −0.629 vs −0.258 and −0.280 vs −0.258 for mode 16 and 0.978 vs 0.335 and 0.582 vs 0.335 for mode 17). In most cases, both contributions have approximately the same relative importance, and can either go in the same direction or in opposite directions. Taking only one of these contributions into account can therefore give rise to completely misleading conclusions. A closer examination of Table 1 shows that, as expected, the total solvent effect is not an additive sum of the direct and indirect effects.

As described in section II, our approach also accounts for "cavity field" and electronic nonequilibrium effects: the relevant data are also collected in Table 1. The results labeled "noncf" have been obtained without cavity field corrections (included in all other calculations), and the label "static" denotes equilibrium solvation in the calculation of the optical tensors (in all other calculations nonequilibrium solvation has been used). The data should be compared with the column denoted (sol,sol). The results obtained with or without cavity field effect are in general close to each other. There are, however, some exceptions, most notably the low-frequency modes (such as mode 22, which is O−C−C bending vibration), where even the sign of the intensities differs. The difference between ROA intensities calculated using equilibrium and nonequilibrium solvation is larger than the effects of the cavity field correction: in many cases (such as modes 1 and 9) solvent shifts obtained using

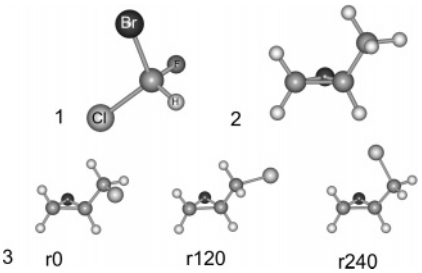

Figure 1. The molecules under investigation: (1) (*R*)-bromochlorofluoromethane; (2) (*S*)-methyloxirane; (3) the three conformers of (*S*)-epichlorhydrin.

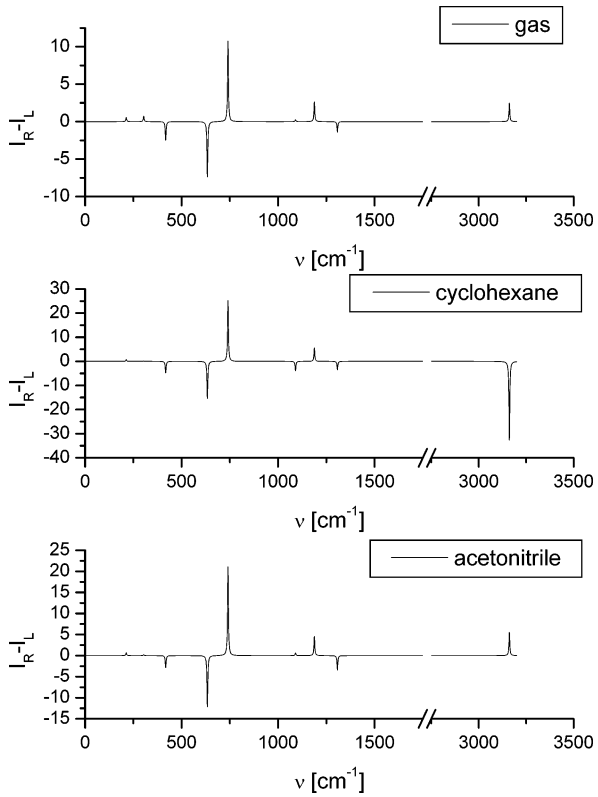

Figure 2. VROA spectra of (*R*)-bromochlorofluoromethane in the gas phase and in cyclohexane and acetonitrile solutions. The ROA differential scattering intensities are in arbitrary units.

equilibrium solvation are qualitatively wrong when compared with those obtained using the nonequilibrium scheme. In all other calculations we have included nonequilibrium solvation and cavity field effects, as well as direct and indirect solvation effects.

The calculated ROA spectra of (*R*)-bromochlorofluoromethane and (*S*)-methyloxirane are shown in Figures 2 and 3, respectively, for gas phase, cyclohexane and acetonitrile. Note that they were obtained by representing each ROA band as a Lorentzian-shaped curve with a half-width of 5 cm^{-1}.

The ROA spectrum of bromochlorofluoromethane in gas phase has already been investigated by Polavarapu and coworkers:[59,60] for this reason we will not discuss it any further. Solvent effects, see Figure 2, are quite substantial for some vibrations, and practically negligible for the others. In particular, the sign of the peak associated with the C−H stretching vibration (mode 1 when numbering the modes according to decreasing wavenumbers) is positive in gas phase, strongly negative in cyclohexane and positive again in acetonitrile. In contrast, the scattering intensity difference of the C−H bending vibration (mode 2) remains practically constant, as does the scattering

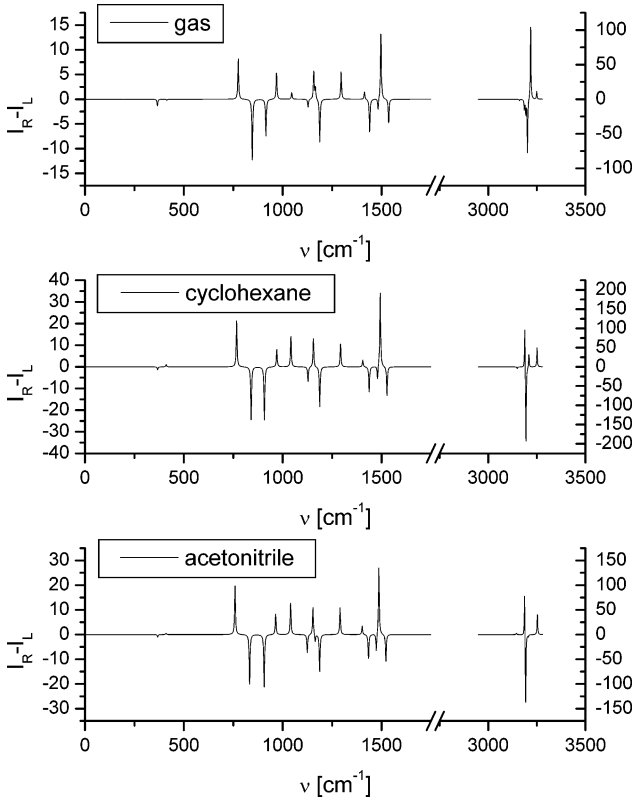

Figure 3. VROA spectra of (*S*)-methyloxirane in the gas phase and in cyclohexane and acetonitrile solutions. The ROA differential scattering intensities are in arbitrary units.

intensity difference of the deformation vibration (mode 3). These findings show that there is no straightforward correlation between solvent polarity and changes in the scattering intensity difference between right and left circularly polarized light.

The ROA scattering intensity differences of methyloxirane (Figure 3) change quite significantly with a change of the dielectric medium, and the direction and magnitude of the solvent effects vary with the spectral region. The ROA scattering intensity differences of the C−H stretching vibrations are sensitive to the environment: for instance, the scattering intensity difference of mode 2, large and positive in the gas phase becomes smaller in cyclohexane and negative in acetonitrile. The scattering intensity differences of mode 5, which is also a C−H stretching vibration, shows an opposite behavior, being small and negative in the gas phase but relatively large and positive in acetonitrile. In the remaining region of the ROA spectrum only small changes are observed. Some of the low-frequency deformation and skeletal bending modes (in particular those with the three lowest frequencies) tend to increase their ROA activity with solvent polarity, but otherwise the solution spectra remain similar to that in gas phase.

The last system studied here is (*S*)-epichlorhydrin. Because of the presence of the chlorine atom, there exist three conformations for this molecule, obtained by rotation of the $-CH_2Cl$ group around the C−C bond (that is, by changing the Cl−C−C−O dihedral angle). In Table 2, the Cl−C−C−O dihedral angles, relative energies, and Boltzmann populations at 298 K of the three conformers are reported in the gas phase and in cyclohexane and acetonitrile.

For the gas phase, r120 is very close in energy to the global minimum r0: the energy difference, as calculated at the B3LYP/cc-pVTZ level, is only 1.85 kJ/mol (2.65 when the zero-point vibrational correction is accounted for). The other structure, r240, is less stable, the energy difference being 6.82 kJ/mol (or

TABLE 2: Dihedral Angles (θ, deg), Relative Energies (ΔE, kJ/mol) and Boltzmann Weights (Bf) of the Three Conformers of Epichlorhydrin in the Gas Phase, in Cyclohexane, and in Acetonitrile

	gas				cyclohexane				acetonitrile			
conformer	θ	ΔE	ΔE_0[a]	Bf[b]	θ	ΔE	ΔE_0[a]	Bf[b]	θ	ΔE	ΔE_0[a]	Bf[b]
r0	162.03	0	0	0.72	161.93	0	0	0.52	161.82	2.19	2.28	0.27
r120	−83.08	1.85	2.65	0.25	−81.90	0.66	0.49	0.43	−79.44	0	0	0.68
r240	51.54	6.82	7.68	0.03	50.72	6.07	5.99	0.05	48.78	6.19	6.21	0.05

[a] ΔE_o includes zero-point vibrational energy. [b] Calculated on the basis of ΔE_o.

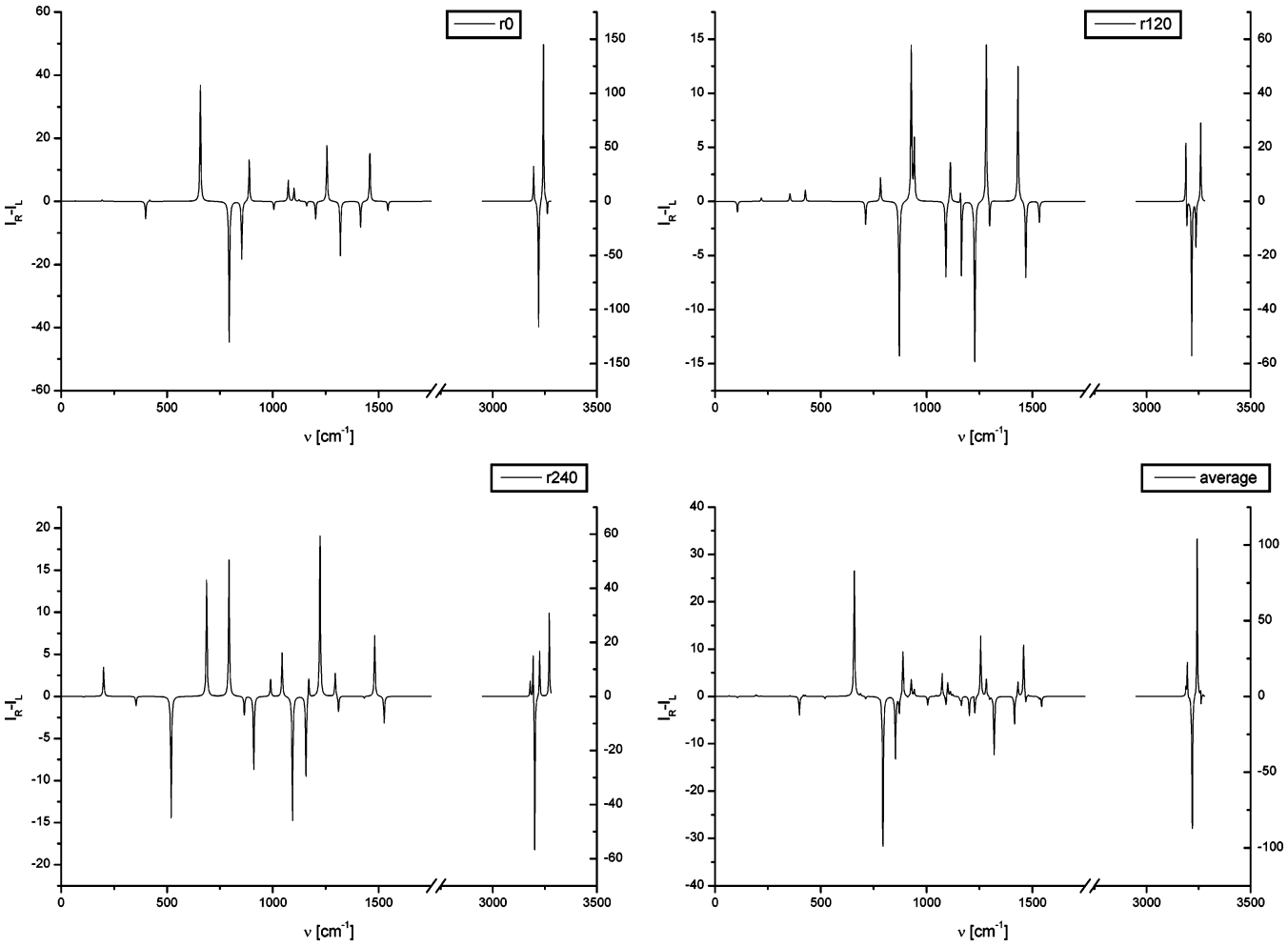

Figure 4. VROA spectra of the three conformations of (*S*)-epichlorhydrin in the gas phase, together with their Boltzmann average. The ROA differential scattering intensities are in arbitrary units.

7.68 kJ/mol, respectively). In cyclohexane, the situation is similar except that r120 is even closer energetically to r0 than in the gas phase. The relative stabilities of r0 and r120 are reversed in acetonitrile, where r120 becomes the global minimum, separated from r0 by more than 2 kJ/mol. For both solvents, r240 is closer to the more stable minimum than in the gas phase, but its Boltzmann weight is still practically negligible. The relative stability of the conformers is not affected by zero-point vibrational energy corrections. The total ROA spectrum is determined by a superposition of the spectra of the r0 and r120 structures, since their Boltzmann weights are comparable. Given the energetic proximity of the two lowest minima, we can expect what we may call a tertiary solvent effect: In addition to the influence on the geometry and on the optical tensors, the presence of a solvent changes also the relative energy of the conformers (reversing the stability of the conformers in the case of acetonitrile), thereby changing the averaged ROA spectrum.

The calculated ROA spectra of the three conformers of epichlorhydrin in gas phase and the Boltzmann average of the spectra are shown in Figure 4. In agreement with earlier studies,[16] the ROA spectrum is very sensitive to the conformation. The spectra of r0 and r120 in particular are very different, especially in the region of C−H stretching vibrations. Considering the changes in the Boltzmann weights of the individual conformers in the different solvents, large solvent effects can be expected on the overall ROA spectra. This is indeed found to be the case, as can easily be seen by comparing the Boltzmann-averaged spectra in Figures 4−6. The most striking change in the Boltzmann-averaged spectrum in cyclohexane (Figure 5) as compared to the one in gas phase (Figure 4) is the decay of ROA activity of the modes at 794 and 658 cm^{-1} (the wavenumbers in the gas phase), which are significant in gas phase. This change is due to a decrease of ROA activity of these modes in the r0 conformer. The solvent-induced changes of the ROA differential intensity of the C−H stretching vibrations have a similar origin: the change of sign for the highest frequency mode in the averaged spectrum is a reflection of an analogous change in the spectrum of the r0 conformer.

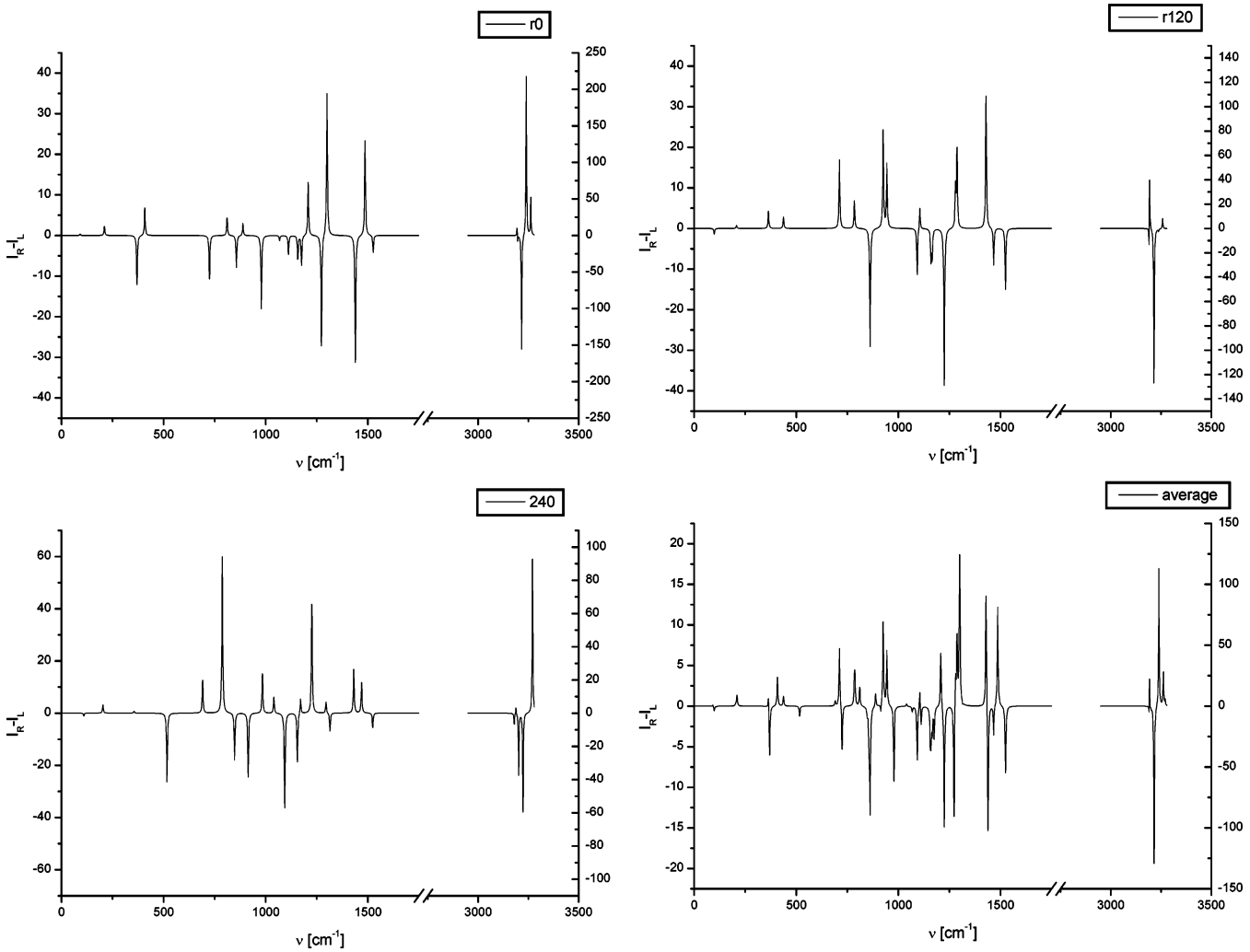

Figure 5. VROA spectra of the three conformations of (*S*)-epichlorhydrin in cyclohexane, together with their Boltzmann average. The ROA differential scattering intensities are in arbitrary units.

The Boltzmann-averaged spectrum of epichlorhydrin in acetonitrile (Figure 6) is again determined by the interplay of solvent effects in the r0 and r120 conformers. The r0 conformer contributes significantly to the ROA scattering intensity difference of the C−H stretching vibrations, as was the case in cyclohexane solution, due to a larger scattering intensity differences of these vibrations for r0 than for the other conformers. For the remaining region, the r120 conformer contributes somewhat more than the r0 one due to its larger Boltzmann weight (in this case, the range of differential intensity is similar for both conformers). The comparison of the spectrum in acetonitrile with those in cyclohexane and the gas phase reveals that, apart from the high-frequency region of C−H stretching vibrations, the solvent-induced changes on the ROA spectrum seem to be rather difficult to analyze, while the ROA scattering intensity differences of the C−H stretching vibrations decrease visibly in acetonitrile.

We end this section by comparing the solvent-induced changes on the ROA scattering intensity differences for the individual conformations. The situation for epichlorhydrin is similar to that already observed in the case of methyloxirane. The ROA spectrum of r0 (compare Figures 4−6) is sensitive to the influence of the dielectric environment. Among the C−H stretching vibrations, mode 1 (asymmetric stretching of the methylene group) changes sign when going from the gas phase to the solvent, and mode 5 (symmetric stretching of the C−H bonds in the $-CH_2Cl$ group) becomes negligible due to the presence of the solvent. In the range between 700 and 1200 cm^{-1} the signs of the scattering intensity differences are changed for many of the vibrational modes. The largest changes are mostly observed when moving from gas phase to either cyclohexane or acetonitrile, whereas the spectra in the two solvents are relatively similar for this conformation.

V. Summary and Conclusions

The IEFPCM (integral equation formalism polarizable continuum model) has been applied to model the solvent effects on Raman optical activity spectra. The "local field" approach has been employed—that is, the "effective" field experienced by the molecule in the cavity has been treated as a sum of a reaction field term and a cavity field term. The response of the solvent to the external field-induced oscillation in the solute electronic density has been treated as dynamic (nonequilibrium). This approach has been used to simulate the effects of solvation on bromochlorofluoromethane, methyloxirane, and epichlorhydrin by cyclohexane and acetonitrile.

The most important observation from the numerical application can be summarized as follows: The solvent-induced changes in the ROA spectrum can be separated into "indirect" changes (resulting from solvent influence on the molecular geometry and molecular Hessian) and "direct" changes (resulting from solvent influence on optical tensors) effects. Our results show that it is essential to account for both of these contribu-

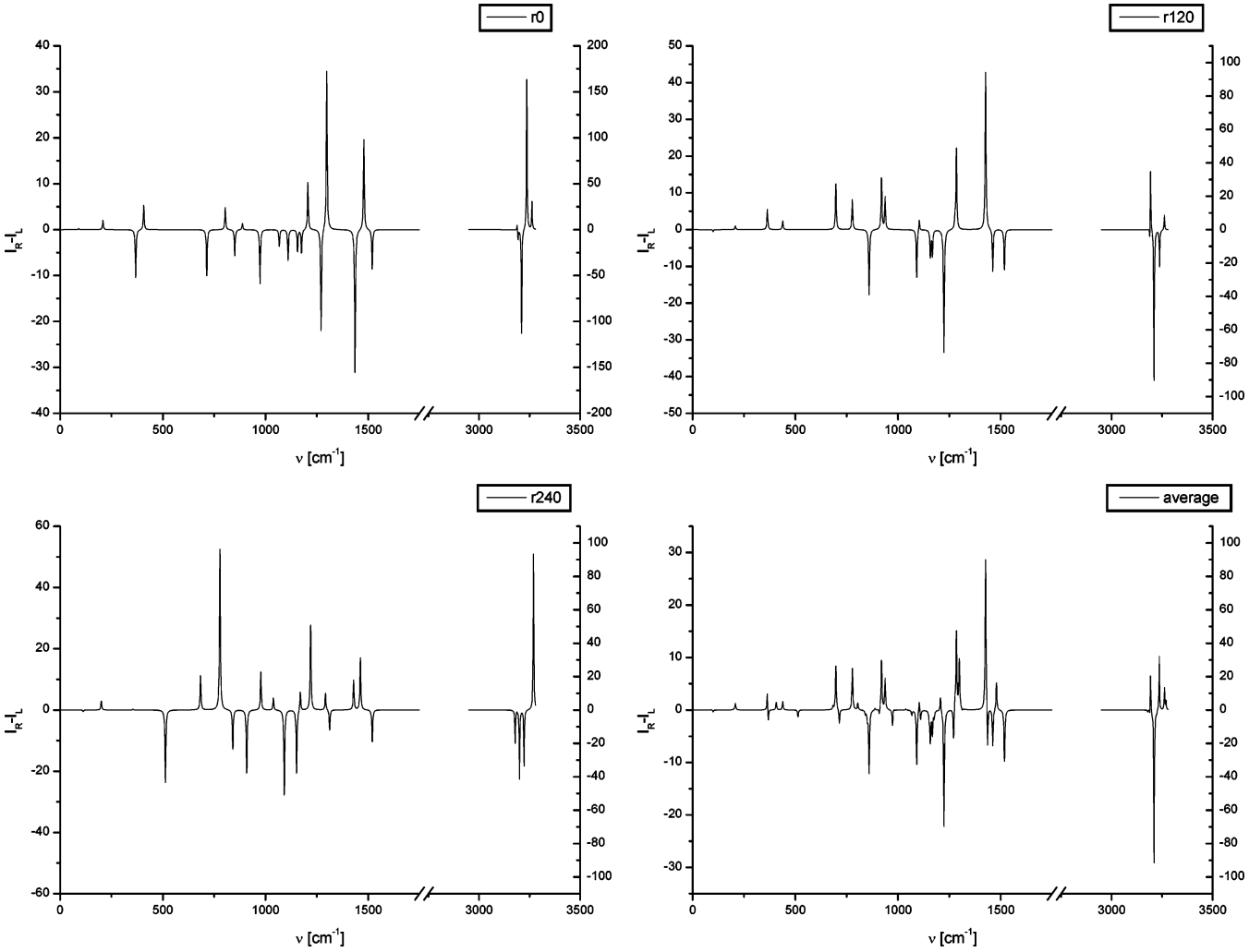

Figure 6. VROA spectra of the three conformations of (*S*)-epichlorhydrin in acetonitrile, together with their Boltzmann average. The ROA differential scattering intensities are in arbitrary units.

tions, as taking only one of them into account can lead to wrong conclusions, such as a wrong sign of the solvent effect. Whereas the use of nonequilibrium solvation (electronic nonequilibrium) seems important, the results obtained with or without cavity field effects—that is, with the "local field" approach or without it—are in general close to each other.

For all three molecules studied here, the most visible solvent effects are observed on the ROA scattering intensity differences of the C−H stretching vibrations. For epichlorhydrin, which is a conformationally flexible molecule, the solvent-induced changes are also caused to some extent by the changes in Boltzmann populations of the individual conformers in different environments. Our findings show that there is no straightforward correlation between solvent polarity and changes in the scattering intensity differences between right and left circularly polarized light.

Acknowledgment. This work has received support from the Norwegian Research Council through a Strategic University Program in Quantum Chemistry grant (Grant No. 154011/420), a YFF grant to K.R. (Grant No. 162746/V00), and Grant Nos. 1T09A07130 MEiN and 120000-501/68-BW-1681/12/05 to M.P. as well as through a grant of computer time from the Norwegian Supercomputing Program. Support from Nordisk Forskarakademi (NorFa Grant No. 030262) is also gratefully acknowledged.

References and Notes

(1) Pecul, M.; Rizzo, A. *Mol. Phys.* **2003**, *101*, 2073.
(2) Zuber, G.; Hug, W. *J. Phys. Chem. A* **2004**, *108*, 2108.
(3) Barron, L. D.; Gargaro, A. R.; Hecht, L.; Polavarapu, P. L. *Spectrochim. Acta* **1991**, *47a*, 1001.
(4) Yu, G.-S.; Freedman, T. B.; Nafie, L. A.; Deng, Z.; Polavarapu, P. L. *J. Phys. Chem.* **1995**, *99*, 835.
(5) Ruud, K.; Helgaker, T.; Bouř, P. *J. Phys. Chem. A* **2002**, *106*, 7448.
(6) Reiher, M.; ;Liegeois, V.; Ruud, K. *J. Phys. Chem. A* **2005**, *109*, 7567.
(7) Pecul, M.; Ruud, K. *Int. J. Quantum Chem.* **2005**, *104*, 816.
(8) Barron, L. D.; Hecht, L.; Bell, A. F. *Appl. Spectrosc.* **1996**, *50*, 619.
(9) Buckingham, A. D. *Faraday Discuss.* **1994**, *99*, 1.
(10) Barron, L. D.; Ford, S. J.; Bell, A. F.; Wilson, G.; Hecht, L.; Cooper, A. *Faraday Discuss.* **1994**, *99*, 217.
(11) Polavarapu, P. L.; Deng, Z. *Faraday Discuss.* **1994**, *99*, 151.
(12) Jalkanen, K. J.; Elstner, M.; Suhai, S. *J. Mol. Struct. (THEOCHEM)* **2004**, *675*, 61.
(13) Barron, L. D.; Hecht, L.; McColl, I. H.; Blanch, E. W. *Mol. Phys.* **2004**, *102*, 731.
(14) Kumata, Y.; Furukawa, J.; Fueno, T. *Bull. Chem. Soc. Jpn.* **1970**, *43*, 3920.
(15) Müller, T.; Wiberg, K. B.; Vaccaro, P. H. *J. Phys. Chem. A* **2000**, *104*, 5959.
(16) Pecul, M.; Rizzo, A.; Leszczynski, J. *J. Phys. Chem. A* **2002**, *106*, 11008.
(17) Miertuš, S.; Scrocco, E.; Tomasi, J. *J. Chem. Phys.* **1981**, *55*, 117.
(18) Mennucci, B.; Cancés, E.; Tomasi, J. *J. Phys. Chem. B* **1997**, *101*, 10506.
(19) Tomasi, J.; Mennucci, B.; Cammi, R. *Chem. Rev.* **2005**, *105*, 2999.

(20) Cappelli, C.; Mennucci, B.; Tomasi, J.; Cammi, R.; Rizzo, A.; Rikken, G. L. J. A.; Mathevet, R.; Rizzo, C. *J. Chem. Phys.* **2003**, *118*, 10712.
(21) Cappelli, C.; Mennucci, B.; Cammi, R.; Rizzo, A. *J. Phys. Chem. B* **2005**, *109*, 18706.
(22) Pecul, M.; Ruud, K. *Magn. Reson. Chem.* **2004**, *42*, S128.
(23) Mennucci, B.; Tomasi, J.; Cammi, R.; Cheeseman, J. R.; Frisch, M. J.; Devlin, F. J.; Stephens, P. J. *J. Phys. Chem. A* **2002**, *106*, 6102.
(24) Pecul, M.; Marchesan, D.; Ruud, K.; Coriani, S. *J. Chem. Phys.* **2005**, *122*, 024106.
(25) Cappelli, C.; Corni, S.; Mennucci, B.; Cammi, R.; Tomasi, J. *J. Phys. Chem. A* **2002**, *106*, 12331.
(26) Corni, S.; Cappelli, C.; Cammi, R.; Tomasi, J. *J. Phys. Chem. A* **2001**, *105*, 8310.
(27) Pecul, M.; Ruud, K.; Helgaker, T. *Chem. Phys. Lett.* **2004**, *388*, 110.
(28) Ruud, K.; Zanasi, R. *Angew. Chem., Int. Ed.* **2005**, *44*, 3594.
(29) Kongsted, J.; Pedersen, T. B.; Strange, M.; Osted, A.; Hansen, A. E.; Mikkelsen, K. V.; Pawlowski, F.; Jørgensen, P.; Hättig, C. *Chem. Phys. Lett.* **2005**, *401*, 385.
(30) Jalkanen, K. J.; Nieminen, R. M.; Frimand, K.; Bohr, J.; Bohr, H.; Wade, R. C.; Tajkhorshid, E.; Suhai, S. *Chem. Phys.* **2001**, *265*, 125.
(31) Bour, P.; Kapitán, J.; Baumruk, V. *J. Phys. Chem. A* **2001**, *105*, 6362.
(32) Barron, L.; Buckingham, A. D. *Mol. Phys.* **1971**, *20*, 1111.
(33) Barron, L. D. *Molecular light scattering and optical activity;* Cambridge University Press: Cambridge, U.K., 2004.
(34) Helgaker, T.; Ruud, K.; Bak, K. L.; Jørgensen, P.; Olsen, J. *Faraday Discuss.* **1991**, *99*, 165.
(35) Placzek, G. In *Handbuch der Radiologie*; Marx, E., Ed.; Akademische Verlagsgesellschaft: Leipzig, Germany, 1934; Vol. 6, page 205.
(36) London, F. *J. Phys. Radium* **1937**, *8*, 397.
(37) Marchesan, D.; Coriani, S.; Forzato, C.; Nitti, P.; Pitacco, G.; Ruud, K. *J. Phys. Chem. A* **2005**, *109*, 1449.
(38) Cancès, E.; Mennucci, B.; Tomasi, J. *J. Chem. Phys.* **1997**, *107*, 3031.
(39) Onsager, L. *J. Am. Chem. Soc.* **1936**, *58*, 1486.
(40) Böttcher, C. J. F.; Bordewijk, P. *Theory of Electric Polarization. Vol. II. Dielectric in time-dependent fields*; Elsevier: Amsterdam, 1978.
(41) Cammi, R.; Mennucci, B.; Tomasi, J. *J. Phys. Chem. A* **1998**, *102*, 870.
(42) Cammi, R.; Mennucci, B.; Tomasi, J. *J. Phys. Chem. A* **2000**, *104*, 4690.
(43) Cammi, R.; Cappelli, C.; Corni, S.; Tomasi, J. *J. Phys. Chem. A* **2000**, *104*, 9874.
(44) Cappelli, C.; Corni, S.; Mennucci, B.; Tomasi, J.; Cammi, R. *Int. J. Quantum Chem.* **2005**, *104*, 716.
(45) Cammi, R.; Tomasi, J. *J. Comput.Chem.* **1995**, *16*, 1449.
(46) Olsen, J.; Jørgensen, P. In *Modern Electronic Structure Theory, Part II* Yarkony, D. R., Ed.; World Scientific: Singapore, 1995; p 857.
(47) Cammi, R.; Frediani, L.; Mennucci, B.; Ruud, K. *J. Chem. Phys.* **2003**, *119*, 5818.
(48) Cappelli, C.; Corni, S.; Tomasi, J. *J. Chem. Phys.* **2001**, *115*, 5531.
(49) Cappelli, C.; Corni, S.; Cammi, R.; Mennucci, B.; Tomasi, J. *J. Chem. Phys.* **2000**, *113*, 11270.
(50) Becke, A. D. *J. Chem. Phys.* **1993**, *98*, 5648.
(51) Stephens, P. J.; Devlin, F. J.; Chabalowski, C. F.; Frisch, M. J. *J. Phys. Chem.* **1994**, *98*, 11623.
(52) Dunning, T. H. *J. Chem. Phys.* **1989**, *90*, 1007.
(53) Kendall, R. A.; Dunning, T. H.; Harrison, R. J. *J. Chem. Phys.* **1992**, *96*, 6796.
(54) Woon, D. E.; Dunning, T. H. *J. Chem. Phys.* **1993**, *98*, 1358.
(55) Woon, D. E.; Dunning, T. H. *J. Chem. Phys.* **1994**, *100*, 2975.
(56) Bondi, A. *J. Phys. Chem.* **1964**, *68*, 441.
(57) Barone, V.; Cossi, M.; Tomasi, J. *J. Chem. Phys.* **1997**, *107*, 3210.
(58) Dalton, an ab initio electronic structure program, release 2.0, 2005. See http://www.kjemi.uio.no/software/dalton/dalton.html.
(59) Polavarapu, P. L. *Angew. Chem., Int. Ed.* **2002**, *41*, 4544.
(60) Costante, J.; Hecht, L.; Polavarapu, P. L.; Collet, A.; Barron, L. D. *Angew. Chem., Int. Ed. Engl.* **1997**, *36*, 885.